Journal of Materials Chemistry C

Accepted Manuscript

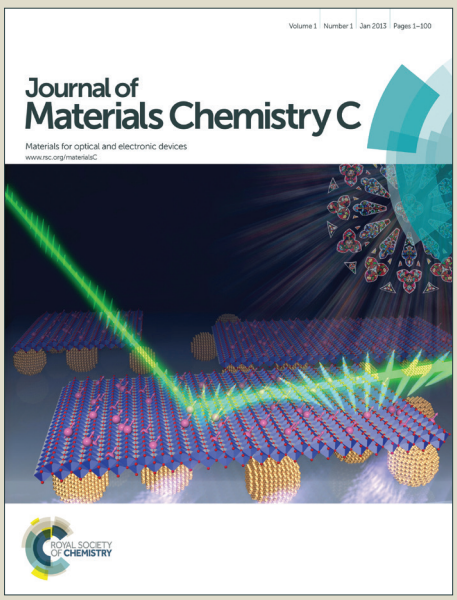

ROYAL SOCIETY OF CHEMISTRY

www.rsc.org/materialsC

Flexible quantum dot-PVA composites for white LEDs

Arzu Coşgun,[1,2] Renli Fu,[1*] Weina Jiang,[1] Jianhai Li,[2] Jizhong Song,[1] Xiufeng Song,[2] and Haibo Zeng[2,1*]

[1]*State Key Laboratory of Mechanics and Control of Mechanical Structures & College of Materials Science and Technology, Nanjing University of Aeronautics and Astronautics, Nanjing 210016, China*

[2]*Institute of Optoelectronics & Nanomaterials (IONS), College of Materials Science and Engineering, Nanjing University of Science and Technology, Nanjing 210094, China*

**Corresponding Emails: zeng.haibo@njust.edu.cn (H. Z.); rlfu@nuaa.edu.cn (R. F.)*

Abstract: Integration of blue light-emitting diode (LED) chips with yellow phosphors has been the most practical way to achieve white lighting, but finding a low-cost alternative for expensive and red-lacked $Y_3Al_5O_{12}$:Ce (YAG) phosphors is still a great challenge. The present report documents a strategy of combining quantum dot-polyvinyl alcohol (PVA) composites and blue chips for white LEDs. Cadmium-free and water-soluble ZnSe:Mn/ZnS quantum dots (QDs) were synthesized through nucleation doping strategy, and then embedded in PVA. The flexible composite contains well-dispersed QDs and exhibits highly efficient photoluminescence at 590 ~ 635 nm, and hence is available for resin-free white LED. Besides excellent stability, the assembled white LEDs possess promising color characters, including color rendering index (CRI) value of 93.5, correlated color temperature (CCT) of 2913 K at Commission Internationale de l'Eclairage (CIE) color coordinates of (0.41,0.37), and luminous efficacy (LE) of 18.9 lm/W under 300 mA current excitation. This work demonstrates that such silica-coated QD-PVA composite plate, as a reliable color converter, would be promising for the next-generation QD-based LEDs.

1. Introduction

Due to high efficiency, long life, low-electricity consumption, fast response time and reliability virtues of white light-emitting diodes (LEDs), there has been greatly increased interest in solid state lighting. Among numerous strategies, integration of blue LED chips with yellow phosphors has been the most practical way. However, as the most popular phosphor, micrometer scale $Y_3Al_5O_{12}$:Ce (YAG) has encountered several obstacles, especially lacking red component in the luminescence of YAG phosphors, which results in lower luminous efficiency and color rendering.[1] Therefore, finding low-cost alternative with better optical properties will greatly advance the development of white lighting, but is still in a great challenge.

In recent years, some novel phosphors, such as organic phosphors with flexibly selected emission color and high efficiency have been reported.[2,3] Nevertheless, the instability and long-term reliability of organic materials are doubtful. In this regard, highly fluorescent quantum dots (QDs) can be considered as the promising scattering-free/scattering-less color converters in white LED fabrication due to their outstanding virtues, such as good photo-stability, high luminescence efficiency and facile color tunability by the quantum confinement effect, and cheap solution processability.[4,5] The development of methods to obtain new low-cost and "green" approaches for a colloidal synthesis of semiconductor quantum dots (QDs) in environment friendly polymers is highly demanded by their potential application in white LEDs. The polymers with embedded QDs structure demonstrate intrinsic properties owing to combination of the inherent characteristics of polymer matrices and unique optical and chemical features of the QDs .[6,7]

Considering recent extensive research activities on light-emitting devices, the polymer is usually used as a production of electroluminescence (EL) devices QD-LEDs, which is one of the major pre-requisites for such devices.[8] However production of electroluminescence (EL) devices QD-LEDs using organic –inorganic charge transport layers experience problems such as high cost and

difficulty of device fabrication.[9] In addition to that, when water-soluble QDs are used ın polymer, usually phase transfer via polymerizable surfactants is necessary.[10]

Herein, a strategy of combining quantum dot-PVA composites and blue chips is developed for white LEDs. Water soluble ZnSe:Mn/ZnS QDs are synthesized through nucleation doping strategy. These QDs are cadmium-free, chemically stable, have high luminescence efficiency. Poly vinyl alcohol (PVA) is chosen as hosting materials in the composite fabrication due to its transparency over the whole visible spectrum, good thermo-stability, chemical resistance, easy processability and good adhesion to hydrophilic surfaces. QD–polymer composite plate is synthesized without unnecessary ligand exchange reaction steps. MPA capped ZnSe:Mn/ZnS quantum dots hydrophilic parts interact with the hydrophobic alkyl chains of PVA. This interaction provided water solubility and chemical functionality[11].The resulting QD/polymer composite materials were easily processable into various shapes and the stability of the photoluminescence properties was improved.

QD-PVA composite plates with QDs uniformly embedded inside PVA matrix are used to fabricate a resin-free White LED. Compared to the colloidal counterparts, the dispersion of QDs in the solid polymer matrix prevents agglomeration very well and makes the storage easier. The formed white LEDs show high luminous efficiency, good stability, and CRI value of 93.5 and CCT of 2913 K at CIE color coordinates of (0.41,0.37).

2.Experimental Procedure

2.1 Preparation of sodium hydrogen selenide

The preparation of NaHSe was performed according to Klayman et al.[12] with some modifications. The presence of $NaBH_4$ and Se in water with a molar ratio of 2:1 , NaHSe was formed according to the reaction equation as follows: $4NaBH_4 + 2Se + 7H_2O \rightarrow 2NaHSe + Na_2B_4O_7 + 14H_2$. All

reactions were performed in oxygen-free water under nitrogen. Briefly, 80.0 mg of $NaBH_4$ was transfered to a small flask which was cooled by ice; then 1 ml H_2O and 79 mg Se powder was put into the flask. A small outlet must be connected to the flask in order to release the pressure from the resulting hydrogen. The black Se powder disappeared and white $Na_2B_4O_7$ precipitation appeared after about 3h. The resulting clear aqueous solution was diluted with 20 mL degassed water and used in the preparation of alloyed ZnSe:Mn-ZnS QDs. We wish to point out that NaHSe solution must be freshly prepared prior to use.

2.2 Preparation of MPA-capped ZnSe:Mn/ZnS QDs

Mn-doped nanocrystals were synthesized by two steps. The first step was the preparation of the ZnSe:Mn core. 0.15 g $ZnSO_4$, 0.008g $Mn(OAc)_2$ and 1.1 g Mercaptopropionic acid (MPA) were loaded into a 100 ml three-necked flask and the pH of the mixture was adjusted to 10 by dropwise addition of a 2 M NaOH solution. After degassing for 1h under N_2 atmosphere, 10 mL of a freshly prepared NaHSe solution were injected dropwise within 5 min into the reaction flask at room temperature, and then mixture was heated to 100°C for 15 h nitrogen flow with a condenser attached until the ZnSe:Mn core QD growth (Supplementary Fig. S1). The purification of these ZnSe cores was needed before the second step. For the shelling reaction, 0.87 mg $Zn(OAc)_2$ $2H_2O$ solution and 0.7 mL of MPA and 90 ml water were loaded into a flask and the pH was adjusted to 10.3 with 4 M NaOH, and the solution was saturated with argon by bubbling for 1h. At the same time, 40 mg of ZnSe:Mn QDs and 65 mL of water transferred into a three-necked flask and purged by argon bubbling for 1h. Then, 25 mL of the Zn^{2+} MPA complex were added dropwisely to the ZnSe:Mn solution and the mixture was heated at 100°C for 6h (Supplementary Fig. S2). As-synthesized ZnSe:Mn /ZnS QDs were precipitated with an excess of ethanol, purified repeatedly with a solvent ethanol by centrifugation (10000 rpm/5 min).

2.3 Preparation of silica coated QD–(PVA) composite plate

The PVA thin film was prepared as follows: white PVA powder (5 g, 0.11 mol) was dissolved in de-ionized water and stirred at 90 °C until a viscous transparent solution was obtained. Then 2.5 ml purified ZnSe:Mn/ZnS QD aqueous solution was added into PVA aqueous solution for 4 h at room temperature (RT). Then, this clear and viscous QD–PVA solution was poured cautiously into a disposable glass dish (50 mm diameter × 10 mm depth), placed in an oven preheated to 25–30°C, and dried under a low vacuum (~66 kPa) for 24 h. The solidified QD–PVA plate was readily detached from the glass dish without damage. To coat the resulting QD–PVA plate with an inorganic passivation layer of sol–gel-derived silica, silica sol was prepared by mixing and reacting 1 ml of tetraethylorthosilicate (TEOS), 10 ml of ethanol, and 1 ml of 0.5 M HCl aqueous solution at RT for 4 h. The QD–PVA plate was simply dip-coated with the above silica sol, and this was followed by drying at 30 °C for 1 h.

2.4 Fabrication of ZnSe:Mn/ZnS QD-based LED devices

In order to make practical devices, NC-doped silica films were coated on InGaN-based UV LED chips (λ_{peak} = 365nm, Epileds co. LTD, Taiwan). First, silica-coated QD–PVA plates were diced to a size similar to the LED chip and placed on top of the chip. Secondly, this chip was placed on a hot plate at 90◦ C for 1 h, for assured that homogeneously distributed on the surface, and finally left for drying for 1 h at room temperature.

2.5 Characterizations

Absorption and photoluminescent (PL) emission spectra of ZnSe:Mn, ZnSe:Mn/ZnS QDs were collected via UV–visible absorption spectroscopy (Shimadzu 3600 UV-Vis spectrophotometer and Varian Cary Eclipse instrument), respectively. PL quantum yields (QYs) of the respective QDs were calculated by comparing their integrated emissions with that of a rhodamine 6G reference dye (QY of 23.5) ethanol solution with an identical QD of ~0.05 at 450 nm. The QY values were determined from the following equation:

$$QY_{Sample} = \frac{F_{sample}}{F_{ref}} \quad \frac{A_{ref}}{A_{sample}} \quad \frac{n_{sample^2}}{n_{ref^2}} QY_{ref}$$

where F, A and n are the measured fluorescence (area under the emission peak), absorbance at the excitation wavelength and refractive index of the solvent respectively. PL spectra were spectrally corrected and quantum yields were determined relative to Rhodamine 6G (QY = 94%). [13]

X-ray diffraction (XRD, D8 Advance from Bruker) using Cu K α radiation was utilized to collect information on the crystal structure and size of the QDs. Transmission electron microscopy (TEM, FEI Tecnai G20) images were taken by placing a drop of the particles in water onto a carbon film-supported copper grid. The thicknesses of the QD–PVA plate and silica over layer were measured using a scanning electron microscopic (SEM, Quanta 250 FEG) operating at 20 kV. The spatial distribution of QDs in the QD–PVA plate was mapped using an energy dispersive spectroscopy (EDX, AZtec X-Max 80 TLE)-equipped SEM operating at 20 kV. LE, CCT, CIE, and CRI of the QD-based LEDs were measured by using an integrating sphere with a diode array rapid analyzer system.

3. Results and discussion

Usually, the phosphors are packed with epoxy or silicone resin in the white LEDs. However, such conventional LED fabrication method contains serious disadvantages.[14] The first one is that, cured epoxy resins are usually hard and brittle owing to rigid cross-linked networks. Secondly, insufficient dispersion compatibility between the LED encapsulant (i.e., silicone resin) and the hydrophobic phosphor surface gives rise to serious agglomerates, which usually results in luminescent quenching and decreased luminescent efficiency.[15] The third disadvantage is called encapsulant yellowing, that epoxy resins degrade under exposure to radiation and high temperatures, resulting in chain scission (which results in radical formation) and discoloration (due

to the formation of thermo-oxidative cross-links).[16] In order to overcome the disadvantages stated above, searchers were fabricated silica composite with embedding individual or multiple QDs in it. During the silica capping process, however, the original QYs are typically not retained and become substantially reduced, presumably due to the chemical attack of the QD surface by water and the catalyst used in the sol-gel reaction.[17] Therefore, fabrication of highly luminescent QD composite, replacing QD-resin, is very promising for single-chip white LEDs, but still a great challenge up to now.

Here, the designed strategy for white LED is presented in Scheme 1. Firstly, highly luminescent manganese-doped zinc selenide (ZnSe:Mn) QDs were synthesized at 100°C using the nucleation-doping strategy. Secondly, overcoating with a large bandgap ZnS shell around the ZnSe:Mn core was applied to improve PL properties. Thirdly, PVA thin film filled with QDs were prepared with suitable ratio (Supplementary Fig. S3), and then coated with a sol–gel-process silica overlay. Finally, silica-coated plate was set on top of 365 nm UV GaInN chip. In many aspect silica coated water soluable QD embedded hybrid PVA structure have advantages in order to reduce the problem mentioned above.

XRD pattern of the Mn:ZnSe and Mn:ZnSe/ZnS core/shell QDs are presented in Figure 1a. For the Mn:ZnSe cores, XRD patterns exhibited characteristic peaks at 27.5°, 45.6° and 54.3° corresponding to the (111), (220) and (311) reflecting planes of cubic zinc blende (JCPDS Card N° 80-0021) nanocrystals, respectively. The diffraction peaks of the Mn:ZnSe QDs exhibit a shift to larger angles compared to the bulk ZnSe material, that is probably due to the deposition of the sulfur on the surface of the Mn:ZnSe QDs with the decomposition of the S-containing MPA.[18] Compared with the Mn:ZnSe core QDs, the diffraction peak positions of the Mn:ZnSe/ZnS core/shell QDs exhibit a slight shift to higher angles toward pure ZnS nanocrystals, that indicates the formation of ZnS shell.[19] According to the Scherrer formula, the average particle sizes of Mn:ZnSe cores and Mn:ZnSe/ ZnS core/shell QDs, estimated from the diffraction line broadening,

are 4.3 and 5.7 nm, respectively. The results are supported by the following TEM results very well. The insert TEM image of QDs in Figure 1b indicated the distances between the adjacent lattice fringes to be 0.33 nm, corresponding to the value for the (111) spacing of ZnSe. The average size of the ZnSe:Mn/ZnS core/shell QDs was 6.0 nm, larger than that of the core QDs, which were about 4.5 nm as shown in Figure 1c. The difference means that the shell thickness is around 1.50 nm. However, because the core and shell have similar electron densities and lattice parameters, the image contrast cannot be used to distinguish them very clearly (Supplementary Fig. S4). EDS (Figure 1d) measurements provide a further proof for the formation of ZnS shell on the Mn:ZnSe cores. Elements of manganese, oxygen, sulfur, zinc, and selenium were clearly detected, which is consistent with the provided components. Carbon and oxygen could be released from the used substrate or the carboxyl groups. The formation of the ZnS shell around the ZnSe cores were clearly demonstrated by increasing Zn/S atomic percantage after formation process. The doping content of Mn is 4.8% based on EDS analysis and it is close to the Mn molar concentration in initial precursors (5%).

Figure 2 presents the evolution of optical properties of ZnSe:Mn QDs after surface-coating with ZnS and then forming composites with PVA. The blue-shift in absorption spectra can be obviously observed from ZnSe:Mn to ZnSe:Mn/ZnS, and to ZnSe:Mn/ZnS PVA QDs, whose band gaps are estimated to be 3.2, 3.62, and 3.75 eV, respectively, as shown in Figure 2a. This 0.5 eV blue-shift is well consistent with the estimated energy change according to quantum confinement effect.The change of band gap can be attributed to the structural change occurring in the nanocomposite and the ZnS (with 3.7 eV band gap) shell effect. Finally, the subtle blue shift in the absorption spectra of the Mn:ZnSe/ZnS–PVA core/shell nanocrystals revealed the formation of a bigger particle size with the doping of the shell of PVA around the ZnSe:Mn/ZnS. The absorption spectrum of MPA capped $ZnSe:Mn^{2+}$ exhibits absorption edge at 390 nm (3.2 eV), which is blue-shifted from that of the bulk ZnSe whose absorption edge is usually located at 460 nm (2.7 eV).[20] Quantum confinement effects

can be observed in transition metal doped group II-VI semiconductors such as ZnS and ZnSe smaller than the Bohr exciton diameter of these materials, ~5.0 nm and ~7.2 nm, respectively.[21,2223] A small absorption peak around 300 to 325 nm appears in ZnSe:Mn/ZnS-PVA's absorption curve because of the characteristics peak of PVA in this region. Similar results were also observed by previous research. It may cause because of the non homegeneous distrubution of QD in PVA.[24]

The photoluminescence spectra of these three typical samples are presented in Figure 2b. The emission of ZnSe:Mn QDs is around 600 nm due to the deep level facilitated by the incorporation of Mn^{2+}.[25] After shell coating, the PL band of ZnSe:Mn/ZnS QDs shifts to 609 nm. Such slight red shift could be induced by the diffusion of partial Mn^{2+} ions from ZnSe cores into ZnS shells due to the higher affinity of Mn^{2+} for ZnS than that for ZnSe and to the concentration gradient.[26] After the dispersing QDs into PVA, the appeared PL centeres at 595 nm and the band departure may originate from the change of surface states. As regarding to the PL intensity, the ZnS-shelled QDs exhibited increased PL intensity compared with the core nano crystals (NCs) due to the surface passivation effect. Furthermore, ZnS shell could make the dopant Mn^{2+} as far as possible from the surface of the NCs, which resulted in emission centers away from the surface trap states, and thereby improved the optical performance with QY of 23.5% .[27] The observed PL QY (23.5) of our ZnSe:Mn/ZnS samples prepared directly in aqueous media is not as high as those (around 40–70%) prepared in organic media,[28,29] but is much higher than that of the previously reported Mn:ZnSe d-dots prepared also in aqueous media. (Supplementary Information -Table 1)

Above explanation is confirmed by PLE spectra. The PLE spectrum of the ZnSe:Mn corresponding to the 600 nm emission exhibits maximum at about 360 nm, indicating the band gap excitation of ZnSe host. After ZnS shell formation, PLE spectra shift to 345 nm, which is the characteristic peak of ZnS absorption. After PVA doping process the emission have shift to 338 nm, in this case the absorption peak is 10 nm blue-shifted in comparison with the branched one due to thicker surface coating.

Several approaches have been reported that the QDs embedded in a polymer can improve the transport properties and increase the efficiency of polymer-based solar cells [30,31] and light-emitting diodes (LEDs). [17,32,33] Here, orange light-emitting ZnSe:Mn/ZnS QDs were used to prepare a QD–PVA composite plate. In order to enhance polymeric coating adhesion, a primer layer of SiO_2 on PVA substrate is deposited by spin coating process. This technique allows an homogenous film elaboration by a controlled parameters, including rotation speed, acceleration, and solution viscosity. And also, the thickness of the plate was readily controllable by varying the PVA and QDs concentration in the mixture solution. As we shown in Figure 3a, QD–PVA composite plate was highly fluorescent under a UV (365 nm) irradiation, and very flexible. Figure 3b presents a typical cross-sectional SEM image of the plate-like composite with the uniform thickness of ~200 μm. Highly smooth surface can be obtained as shown in Figure 3c. The corresponding Zn, Se and Mn elements mapping **(**Figure 3d, 3e and 3f**)** demonstrats that the QDs have been homogeneously dispersed in the matrix without obvious agglomeration.

Regarding the strong oxygen isolation (P^{O2}_{PVA} = 3x $10^{-17}$$cm^3$cm/$cm^2$s Pa compared to P^{O2}_{PET} = 3x$10^{-15}$$cm^3$cm/$cm^2$s Pa) and high transparency properties of PVA, these QD-PVA composites are anticipated to be a good candidate for WLED.[34,35] However, when exposing onto UV irradiation, PVA could restrain PL quantum yield of embedded QDs. [16,18] On the basis of early published results, the strongest point is the high stability of PVA upon irradiation in the absence of oxygen, even after long exposure ,this result is prime importance for the incorporation of PVA in a durable multilayer encapsulation system for WLED as long as the PVA layer is protected from air by an inorganic layer as a first outside layer in the inorganic/ organic multilayer. In this case applying tetraethoxyothosilicate (TEOS) based silica as a inorganic coating layer on the surface PVA would work as a gas barrier layer as shown in the result of EDS results. The silica layer can be conveniently deposited onto the composite plate by a low-cost sol–gel method. As a matter fact, SiOx[36, 37,] SiNx[38], and Al_2O_3[39] layers have been applied in flexible QLEDs in order to act as barriers to environmental O_2 and H_2O. A typical oxygen transmission rate (OTR) value for SiOx can be as

low as 0.5–0.8 $gm^{-2}d^{-1}$ depending on the layer quality. Figure 3g presents the cross-sectional SEM image of the whole multilayer structures. The silica coating thickness is approximately 30 μm. As demonstrated in Figure 3h, the distribution of Si, O and C atoms of hybrid plate, Poly(vinyl alcohol)/SiO_2 hybrid coating materials can provide an improved gas barrier property for the QD contained LED, such gas separation is very crucial for the performance of final LED. These promising results demonstrate that our simple, low-cost solution-processed PVA/silica hybrid barrier layer worked well in effectively hampering the gas permeation into the QD plate. Hybrid WLED was simply constructed by setting of the QD plate on top of InGaN UV chips as a down converter , as schematically depicted in scheme 1.

Figure 4 shows the performance of LED after assembling the silica-coated quantum dot-PVA composite on single InGaN chip. As shown in Figure 4a, owing to the bi-color mixing of UV plus orange with a suitable ratio, white light emission was satisfactorily achieved. Remarkably, the peak intensity of such orange emission can reach at 1/3 of UV peak from underlying chip. Such relatively intensive orange emissions from silica-coated quantum dot-PVA composite are very necessary for the final formation of white light emission. The orange band have peak located at 580 nm, and full-width-at-half-maximums (FWHM) is about 100 nm. The blue and orange emission components increased monotonically to almost the same degree with the input current increasing from 20 to 300 mA without a noticeable blue-shift or QD peak shift. Remote-type W-LED device equipped with the above gas-barrier-coated QD plate was placed in continuous operation at 20 mA for up to 25 h. Figure 4(b) presents the variation of the EL spectra recorded with the elapsing of operating time. In contrast to the results from the bare QD plate-based WLED in Supplementary Fig. S5, the initial peak wavelength remained almost unchanged throughout the 25 h operation period, displaying an exceptionally high spectral stability of the white light generated.

To obtain “warmer” looking light that more closely matches the color quality of incandescent lighting, appropriate down-converters should be implemented to enhance addition of red-emitting QDs to a blue LED coated with a yellow phosphor that improves CRI from about 70 to greater than

90 and lowers CCT to a more desirable 2700 K without greatly reducing the device's luminous efficienc.[40] As shown in Figure 4c, the chromaticity coordinates of the ZnSe:Mn QDs (P1) and ZnSe:Mn/ZnS QDs (P2) are marked to be (0.50, 0.47) and (0.58, 0.41), respectively. After the ZnS shell formation the intensity of the orange light increases as mentioned in the PL graph (Figure 2). The CIE coordinates (P3) of the final LED obtained by combining a 365 nm UV chip with ZnSe:Mn/ZnS-PVA QDs were located at x=0.41 and y= 0.37 with high CRI 93.5, in the range CCT is 2913 K and LE of 18.9 lm/W at 300 mA. On the basis of free-standing QD-PMMA with CIS/ZnS/ZnS shell QDs were synthesized and applied it to QD-WLEDs,[41] regarding to having low CCT, our silica-coated QD plate, as a reliable color converter, should be promising as regards the development of next-generation QD-based LEDs to a practical standard.

Compared to the white LED based on conventional phospho utilizing the PVA ınstead of resin matrix result on well dispersed structure. Secondly the preparation condition requirements for the YAG:Ce ceramic plate required a high sintering temperature of 1780°C maintained for the long time of 20 h however ZnSe:Mn/ZnS quantumd dots synthesis lower temperature and time condition. Due to interactions between QDs and polymer high stability of the photoluminescence properties was obtained. (Supplementary Fig. S5) In addition to these cadmium free QDs embedded PVA plate is a cost effective and environment friendly which can be the good candidate for the future lighting approaches.

4. Conclusion

The low-toxic, highly luminescent Mn:ZnSe/ZnS core/shell QDs were successfully sythesısed in aqueous solution. The obtained results indicate that QDs have good crystallinity and have a emission at 600 nm exhibited an PL QY of 23.5% in water and a diameter of 6 nm. Practical ~200 μm thick, QD–PVA composite plate has been prepared and coated with silica layer. White LEDs were fabricated by combining 365 nm InGaN led chip with silica coated PVA doped NCs. The QD

plate-based WLED showed the high CRI 93.5 at between 20-300 mA. A remote-type WLED equipped with a silica-barrier-coated QD plate displayed high device stability with the elapsing of the operating time up to 25 h along with stable white light qualities regardless of the operating time at a current input of 20 mA.

Acknowledgements

This work was financially supported by the National Basic Research Program of China (2014CB931700), NSFC (61222403), the Doctoral Program Foundation of China (20123218110030), and the Opened Fund of the State Key Laboratory on Integrated Optoelectronics (IOSKL2012KF06).

REFERENCES

1. J. K. Sheu, S. J. Chang, C. H. Kuo, Y. K. Su, L. W. Wu, Y. C. Lin, W.C. Lai, J. M. Tsai, G. C. Chi and R. K. Wu, *IEEE Photon. Technol. Lett*., 2003, **13**, 18.
2. F. Hide, P. Kozodoy, S. P. DenBaars, A. J. Heeger, *Appl. Phys.Lett*., 1997, **70**, 2664.
3. H. Xiang, S. Yu, C. Chea and P. T. Lai, *Appl. Phys. Lett*., 2003, **83**, 1518.
4. X. Wang, W. Li, and K. Sun, *J. Mater. Chem*., 2011, **21**, 8558 .
5. K. Kim, S. Jeong, J. Y. Woo and C. S. Han, *Nanotechnology*., 2012, **23**, 065602 .
6. N. Tomczak, D. Janczewski, M. Han, G.J.Vancso, *Prog. in Poly. Sci*., 2009, **34**, 393.
7. J.C. Ferrer, A. Salinas-Castillo, J.L. Alonso, S. Fernandez de Avila, R. Mallavia, *Mater. Lett*., 2009, **63**, 638.
8. N. Tomczak, D. Janczewski , M. Han , G. J. Vancso, *Progress in Polymer Science.,* 2009, **34,** 393–430
9. S. W. Kim, S. H. Im, S. W. Kim, *Nanoscale*, 2013, **5**, 5205–5214
10. N. Tomczak, D. Janczewski , M. Han , G. J. Vancso, *Progress in Polymer Science.,* 2009, **34,** 393–430
11. X. Gao, L. Yang, J.A. Petros, F.F. Marshall, J.W. Simons, S. Nie, *Curr Opin Biotechnol.*, 2005, **16**, 63–72
12. D. L. Klayman, T. S. Griffin, *J. Am. Chem. Soc*., 1973, **95**, 197.
13. M. Fischer, J. Georges, *Chem. Phys. Lett*., 1996, **260**, 115.

14. S. Nishiura, S. Tanabe, K. Fujioka, and Y. Fujimoto, *Opt. Mater.*, 2011, **33** , 688.
15. W. S Song , H. Yang, *Chem. Mater*., 2012, **24** , 1961.
16. J. Ziegler, S. Xu, E. Kucur, F. Meister, M. Batentschuk, F. Gindele , T. Nann, *Adv. Mater.,* 2008, **20**, 4068.
17. H. Kim, B. H. Kwon, M. Suh, D. S. Kang, Y. Kim, D. Y. Jeon, *Electrochem. Solid State Lett*., 2011**, 14**, 55.
18. A. Aboulaich, M. Geszke, L. Balan, J. Ghanbaja, G.Medjahdi, R. Schneider , *Inorg. Chem.,* 2010**, 49**, 10940–10948. doi:10.1021/Ic101302q
19. D. V. Talapin, I. Mekis, S. Gotzinger, A. Kornowski, O. Benson, H. Weller, *J. Phys. Chem. B.,* 2004, **108**:18826–18831. doi:10.1021/Jp046481g
20. P. E. Lippens, M. Lannoo, *Phys. Rev. B*., 1989, **39**, 10935.
21. N. Pradhan, X. Peng, *J. Am. Chem. Soc*., 2007, **129**, 3339.
22. H. Menkara, R. A. Jr. Gilstrap, T. Morris, M. Minkara, B. K. Wagner, C. J. Summers, *Optics Express*, 2011, **19**, A972
23. H. Zeng, G. Duan, Y. Li, S. Yang, X. Xu, W. Cai*, Advanced Functional Materials*, **2010**,561-572.
24. S. Baoting, S. Xin , W. Ji, C. Daniel, W. Andrew, G. Zhanhu, *Matr. Chem. and Phy*., 2010, **119** , 237–242.
25. S.C. Erwin, L. Zu, M. I. Haftel, A. L. Efros, T. A. Kennedy, D. J. Norris, *Nature*, 2005, **436**, 91.
26. A. Aboulaich, M. Geszke, L. Balan, J. Ghanbaja, G.Medjahdi, R. Schneider, *Inorg. Chem.,* 2010**, 49***,*10940.
27. Z. Dong, J. Xiaoxing, Z. Cuie, S. Xiaolian, Z. Jianrong and J. Z. Jun, *Chem. Commun*., 2010, **46**, 5226.
28. N. Pradhan, D. Goorskey, J. Thessing, X. Peng, *J. Am.Chem. Soc.*, 2005, **127**, 17586.
29. V. Wood, J. E. Halpert, M. J. Panzer, M. G. Bawendi, V. Bulovic, *Nano Lett*, 2009 , **9,** 2367
30. N. Tomczak, D. Janczewski, M. Han, G.J.Vancso, *Prog. in Poly. Scie*. 2009 , **34** 393–430.
31. A.J. Nozik, M. C. Beard, J. M. Luther, M. Law, R. J. Ellingson, J. C. Johnson, *Chem. Rev*., 2010,**110** ,6873.
32. M. Zorn, W. K. Bae, J. K Wak, H. Lee, C.Lee, R. Zentel, K. Char, *ACS Nano*., 2009**, 3** , 1063–1068.
33. V. Wood, V. Bulovic, *Nano Reviews*, 2010, **1**, 5202.
34. T. N. Chen, D. S. Wuu, C. C. Wu, C. C. Chiang, Y. P. Chen and R. H. Horng, *Plasma Processes Polym.*, 2007, **4**, 180.
35. M. S. Weaver, L. A. Michalski, K. Rajan, M. A. Rothman, J. A. Silvernail, J. J. Brown, P. E. Burrows, G. L. Graff, M. E. Gross, P. M. Martin, M. Hall, E. Mast, C. Bonham, W. Bennett , M. Zumhoff, *Appl. Phys. Lett*., 2002, **81**, 2929.
36. S. Iwamori, Y. Gotoh , K. Moorthi, *Surf. Coat. Technol*., 2003, **166***,* 24.

37. D. S. Wuu, T. N. Chen, C. C. Wu, C. C. Chiang, Y. P. Chen, R. H. Horng and F. S. Juang , *Chem. Vapor Depos*., 2006, **12**, 220.
38. J. S. Lewis and M.S. Weaver, *IEEE J. Sel. Top. Quantum Electron*, 2004 , **10** , 45.
39. J. Meyer, P. Corrn, F. Bertram, S. Hamwi, T. Winkler, H. H. Johannes, T. Weimann, P. Hinze, T. Riedl and W. Kowalsky, *Adv. Mater*., 2009, **21**, 1845.
40. P. J. Eun, S. S. Woo, H. L. Ki, Y. Heesun, *Nanotechnology*, 2013**, 24** , 7.
41. D.V. Talapin , J. Steckel, *Material Research Society* , DOI: 10.1557/mrs.2013.204.

FIGURES

Scheme 1

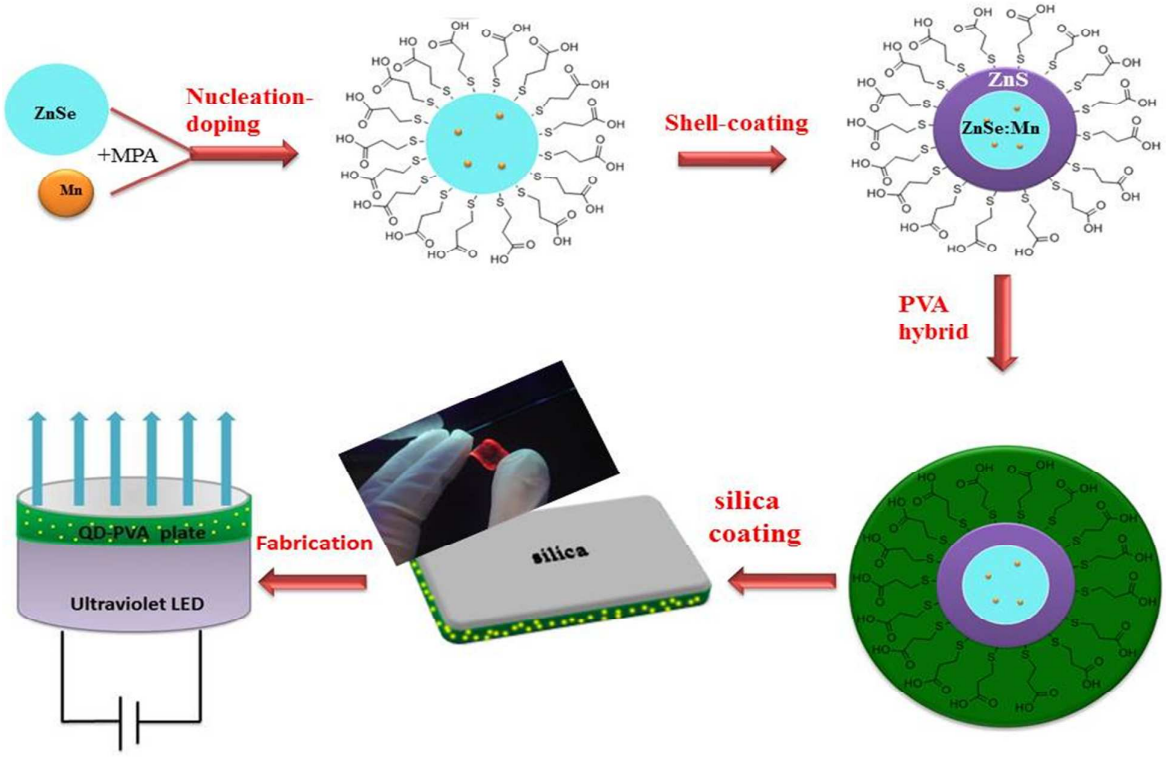

Scheme 1. Fabrication strategy of white light-emitting diodes based on UV light-emitting diodes with silica-coated quantum dot-PVA composites as hybrid phosphors.

Figure 1

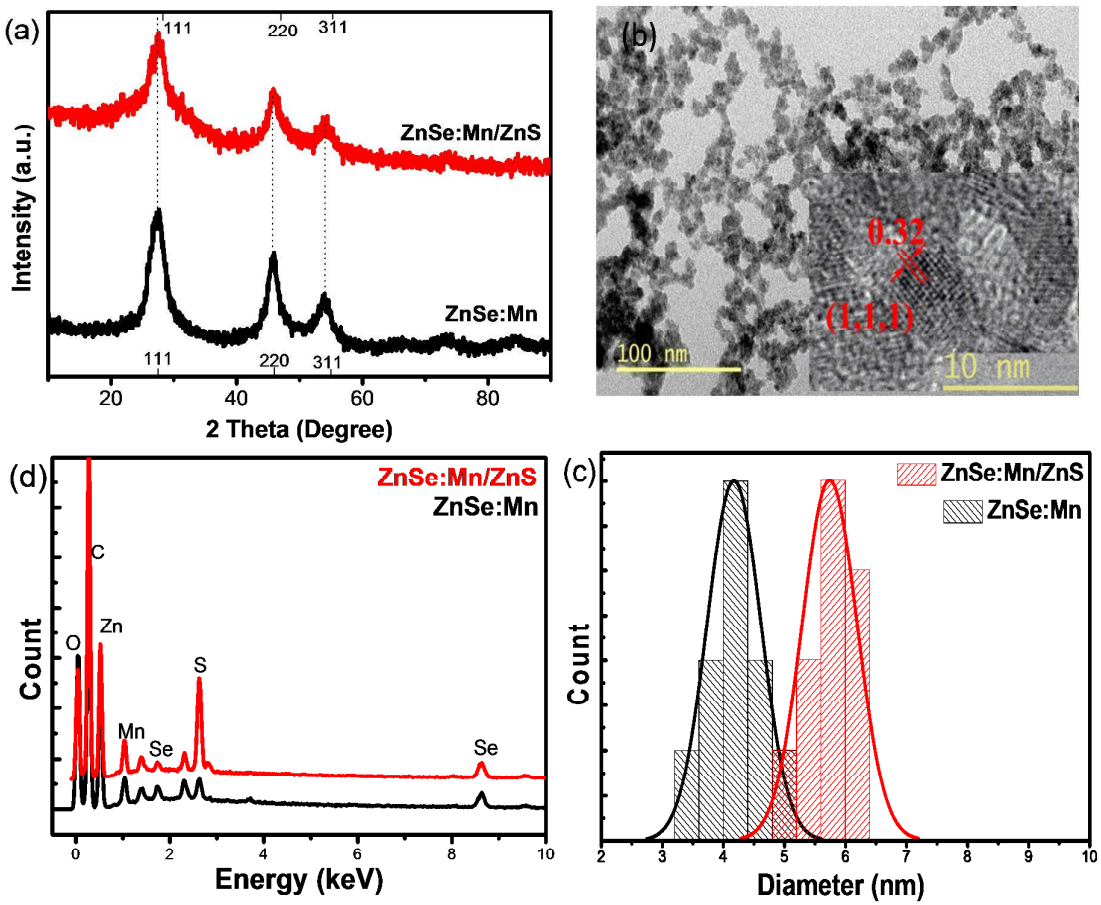

Figure 1. (a) XRD patterns of ZnSe:Mn and ZnSe:Mn/ZnS core/shell QDs. (b) Low- and high-magnification (inset) TEM images of the ZnSe:Mn/ZnS core/shell QDs. (c) Size distribution histogram of ZnSe:Mn/ZnS QDs. (d) EDs spectra of QDs before and after the formation of the ZnS shell.

Figure 2

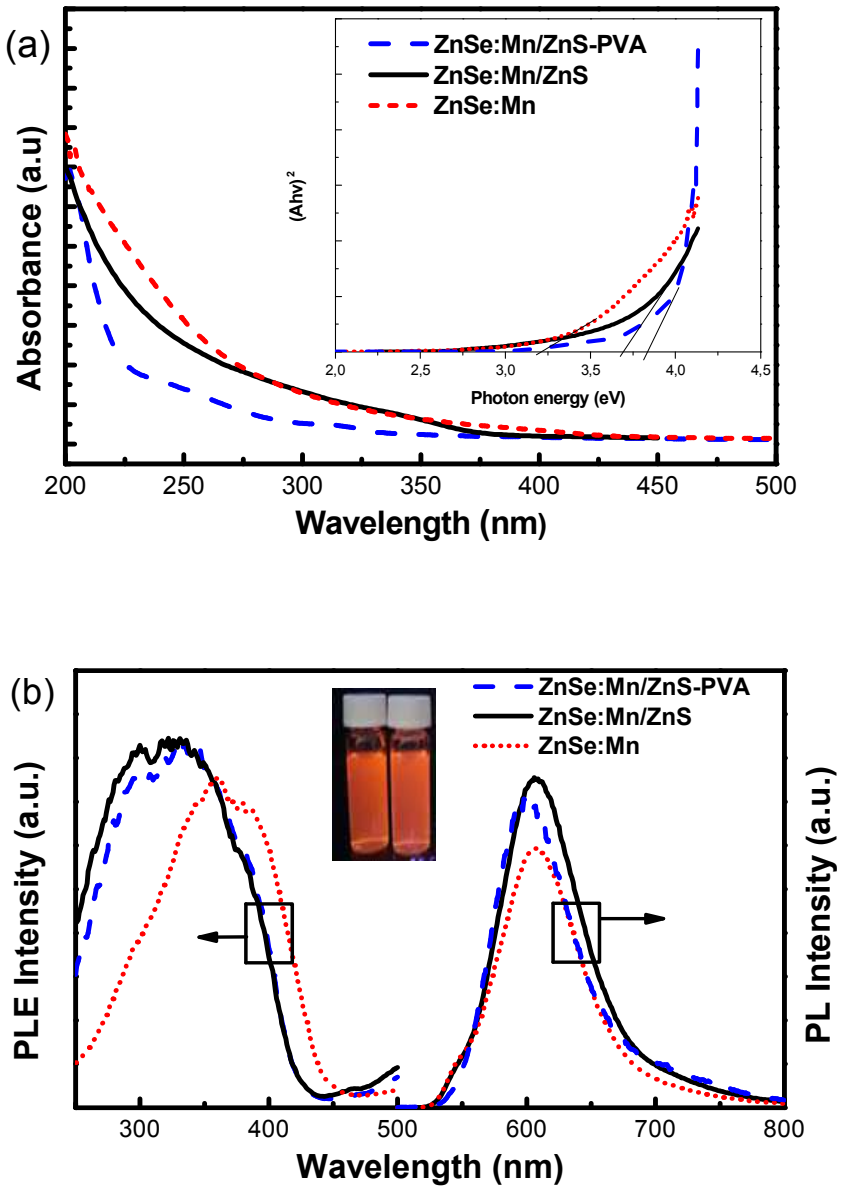

Figure 2. (a) Absorption, (b) PLE and PL spectra of ZnSe:Mn, ZnSe:Mn/ZnS and ZnSe:Mn/ZnS-PVA QDs. The inset shows the corresponding $(Ahv)^2$ versus hν relations. Inset pictures of the QDs before (left) and after (right) the overcoating with ZnS.

Figure 3

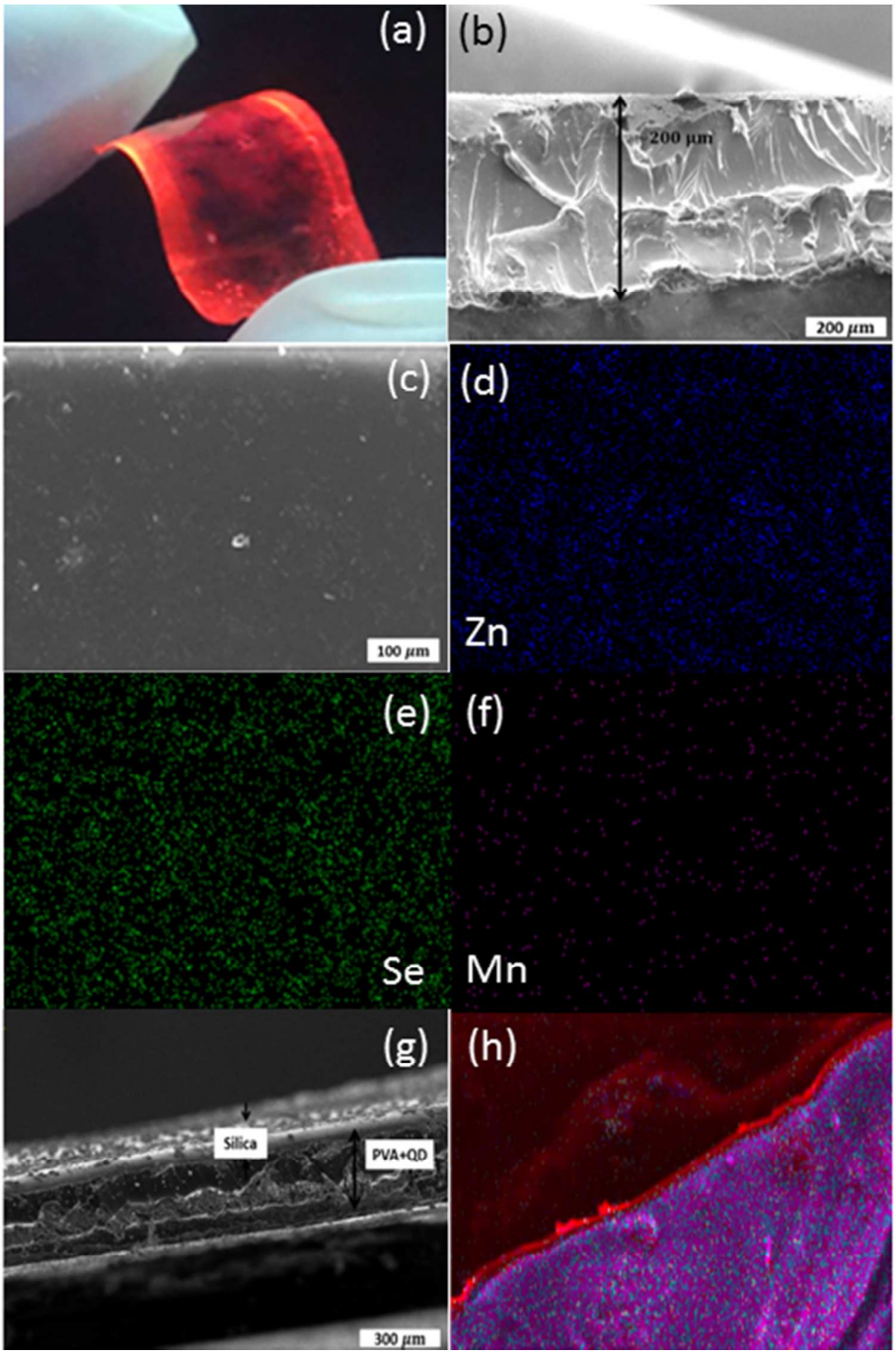

Figure 3. (a) Fluorescent photograph under UV illumination, (b) cross-sectional SEM image, and (c) top-view SEM image of a ZnSe:Mn/ZnS QD-PVA composite plate. (c) Zn Lα, (d) Se Lα, and (e) Mn Lα EDS compositional mapping images of the plate surface (c). (g) Cross-sectional SEM image and (h) corresponding O-Si-C EDS compositional mapping images of the silica-coated QD-PVA composite plate on a LED chip

Figure 4

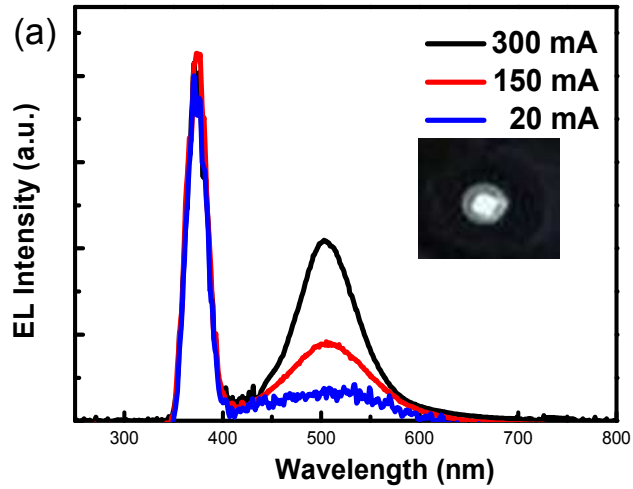

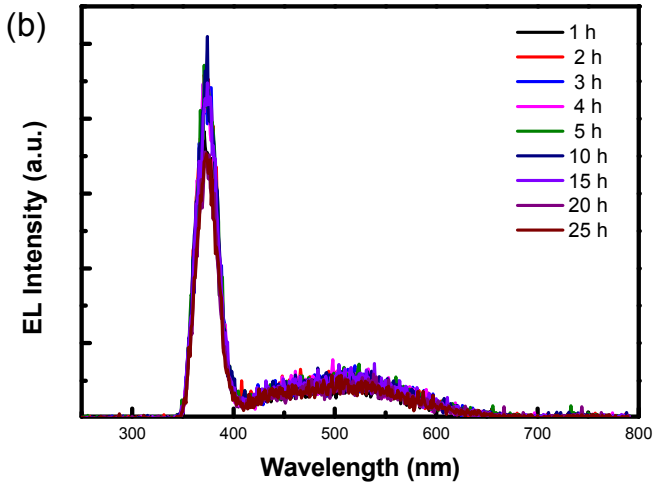

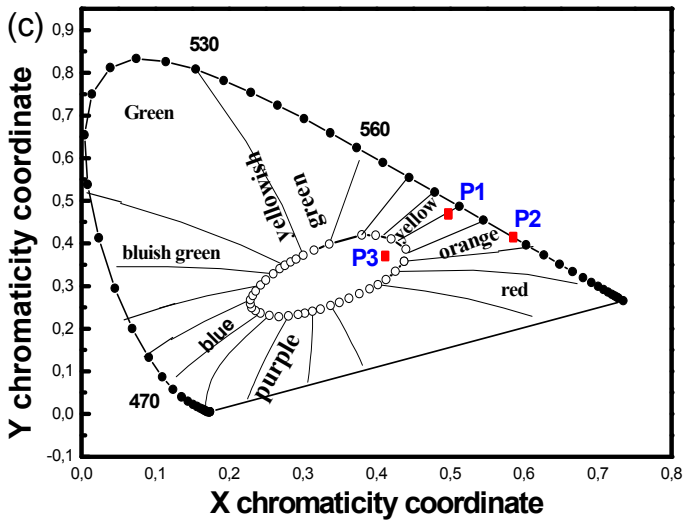

Figure 4. (a) EL spectra of assembled LED constructed with silica-coated quantum dot-PVA composite on single InGaN chip, the inset shows the photograph of a emitting white-LED under a 300 mA input current. (b) Temporal evolution of EL spectra. (c) the corresponding CIE chromaticity diagra

TOC Picture